Generalized Spectral-Domain Analysis for Multilayered Complex Media and High-Tc Superconductor Applications

Zhenglian Cai, *Student Member, IEEE* and Jens Bornemann, *Senior Member, IEEE*

Abstract—**An efficient algorithm to rigorously derive the spectral-domain impedance dyadic Green's function for MMIC's on general complex anisotropic or bi-anisotropic substrates is developed. The main advantage of the applied technique is that it provides closed-form expressions for transverse propagation constants and related immittances in the spectral domain and, therefore, allows the following parameters to be taken into account: dielectric and magnetic losses of anisotropic or bi-anisotropic media without restrictions to the magnitude of tensor elements, alternative directions for magnetic bias, the finite metallization thickness of conventional conductors and/or superconductors including their losses, microstrip and coplanar waveguide structures in open, shielded and conductor-backed technology. The theory is verified by comparison with previously published data. The flexibility is demonstrated for both superconductor and conventional conductor (M)MIC structures on ferrite-dielectric or bi-anisotropic substrates with different directions for magnetic bias. The CPU time is 10–20 seconds per frequency sample on a modern workstation.**

I. Introduction

OWING to the advances in material technology and the steady interest in high-frequency bands, monolithic integrated circuits with anisotropic media are rapidly gaining importance in microwave and millimeter-wave components. Particularly, the wide variety of possible low-loss and low-dispersion applications of high-Tc superconductor-film MMIC's with anisotropic substrates offer attractive solutions in practice, such as in microwave resonators, filters, delay lines and antenna systems, e.g. [1]–[3]. Moreover, many other (M)MIC substrates exhibit anisotropies which are either natural or introduced during the manufacturing process [4].

Different methods utilizing conventional spectral domain approaches (SDA) have been proposed for the analysis of planar layered anisotropic structures. Among those are quasi-static approaches, e.g. [4]–[6], and full-wave solutions, e.g. [7]–[10], all of which emphasize certain aspects but are restricted to either lossless substrates and/or conductors, infinitely thin conductors, magnetic bias in only one direction, purely diagonal material tensors, or single-layered substrates. Although the method proposed by Krowne [11] appears to be the most general one because it includes bi-anisotropic media, it lacks closed-form expressions for the dyadic Green's function. As an alternative, a similar scheme called equivalent boundary method (EBM) is presented by Mesa [12] to derive a bi-dimensional spectral dyadic Green's function—under the assumption, however, of lossless and infinitely thin metallizations. Even most recently published approaches consider only a single dielectric substrate with purely diagonal tensor representation [19], or neglect losses and the finite strip thickness [20].

Therefore, this paper focuses on an algorithm to rigorously derive the impedance dyadic Green's function in the spectral domain. The method is capable of combining the capabilities of many previously presented techniques while preserving enough flexibility to include

- layered anisotropic or bi-anisotropic substrates with either conventional conductor or high-Tc superconductor film
- dielectric and magnetic losses
- the finite metallization thickness and conductor losses via an approximation related to the surface impedance
- the possibility of magnetic bias in x, y, or z direction
- microstrip and conventional as well as conductor-backed coplanar structures requiring boundary conditions, e.g. electric or magnetic walls, in only one cross-sectional dimension, whereas the structure can be open in the other direction.

The method is demonstrated at the examples of layered ferrite and dielectric substrates (both lossy) with practically realistic five- and three-element tensor representations, respectively, and bi-anisotropic substrates with diagonal permeability and permittivity tensors. The consideration of more general tensors seems possible but has not been investigated yet. The proposed algorithm is based on the spectral domain immittance approach (SDIA) [13] combined with the concepts of TE and TM waves for anisotropic substrates. The advantages of this approach are twofold: first, electric and magnetic fields in a lossy

Manuscript received July 10, 1992; revised July 30, 1992.

The authors are with the Laboratory for Lightwave Electronics, Microwaves and Communications, Department of Electrical and Computer Engineering, University of Victoria, Victoria, BC Canada V8W 3P6.

IEEE Log Number 9203680.

anisotropic medium can be decoupled in the spectral domain and, secondly, closed form solutions are derived for the different transverse TE- and TM-wave propagation constants, thus directly determining the impedance dyadic Green's function in the spectral domain. The finite metallization thickness and the conductor losses are included by considering a complex boundary condition approximation [17] which relates to the surface impedance of the conductor.

II. Analytical Formulation

The process to formulate the dyadic Green's function of structures based on ferrite-dielectric (Fig. 1(a)) or bi-anisotropic (Fig. 1(b)) substrates follows the spectral domain immittance approach (SDIA). It results in a simple solution for multilayered structures by decoupling the TE- and TM-wave components. For details regarding the basic concept of SDIA, the reader is referred to [13]. In the case of an anisotropic substrate, however, the key problem is to find closed-form expressions for the wave immittances of transversely propagating TE and TM waves. This procedure is demonstrated below at the examples of a ferrite-dielectric layered and a bi-anisotropic substrate followed by the treatment for the metallization.

1. Ferrite-Dielectric Layered Substrate

For the three different cases of magnetic bias in x, y or z direction (c.f. Fig. 1(a)), the permeability tensor reads:

$$\langle \vec{\mu} \rangle = \mu_0 \begin{cases} \begin{pmatrix} \mu_x & 0 & 0 \\ 0 & \mu & -j\kappa \\ 0 & j\kappa & \mu \end{pmatrix} & H_0 = H_x \\ \begin{pmatrix} \mu & 0 & j\kappa \\ 0 & \mu_y & 0 \\ -j\kappa & 0 & \mu \end{pmatrix} & H_0 = H_y \\ \begin{pmatrix} \mu & -j\kappa & 0 \\ j\kappa & \mu & 0 \\ 0 & 0 & \mu_z \end{pmatrix} & H_0 = H_z \end{cases} \quad (1)$$

where μ and κ as well as the permittivity ϵ (c.f. Fig. 1(a)) are complex quantities to account for the losses in the magnetic and dielectrical materials. Experimental expressions [14]–[15] specify either the scalar permeability or the tensor elements for a demagnetized or partially magnetized/saturated ferrite, respectively.

a) Magnetic Bias in y Direction: Using the concept of SDIA, the six-component electromagnetic field considered in the coordinate system (x,y,z) can be decomposed into TM-to-y and TE-to-y when transformed into a (u,v,y) system [13]. By solving the wave equations in the spectral domain, the related propagation constants $\gamma_{m,e}$ and associated admittances $Y_{TM,TE}$ are obtained

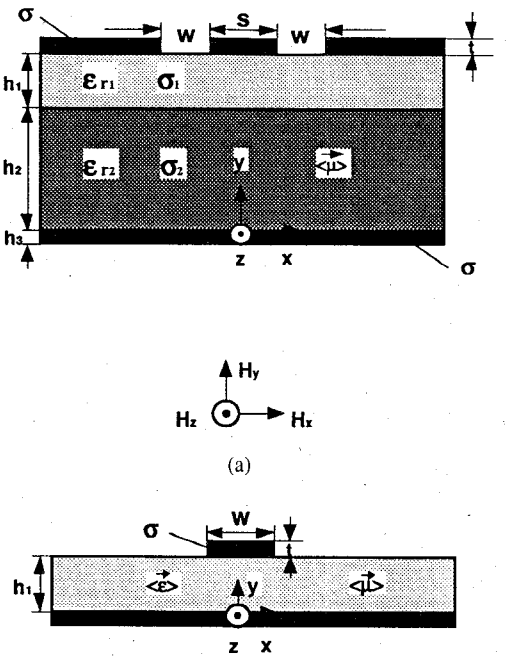

Fig. 1. Cross-sections of MMIC transmission lines. (a) Conductor-backed coplanar waveguide on ferrite-dielectric layered substrate. (b) Microstrip line on bi-anisotropic substrate.

$$\gamma_m^2 = -k_0^2 \epsilon_r \mu_\Delta + \alpha^2 + \beta^2$$

$$\gamma_e^2 = \frac{\mu}{\mu_y}(-k_0^2 \epsilon_r \mu_\Delta + \alpha^2 + \beta^2) \quad (2)$$

$$Y_{TM} = \frac{j\omega\epsilon_0\epsilon_r}{\gamma_m} \qquad Y_{TE} = \frac{\gamma_e}{j\omega\mu_0\mu_\Delta} \quad (3)$$

with

$$k_0^2 = \omega_0^2 \epsilon_0 \mu_0 \qquad \mu_\Delta = (\mu^2 - \kappa^2)/\mu \quad (4)$$

and the propagation constants α, β in x, z directions, respectively [13]. Note that contrary to the treatment given in [16], the propagation constants γ_m and γ_e in (2) differ from each other and, therefore, do not require restrictions such as in [16] on the ratio of tensor elements. With the wave immittances of (3), the elements of the impedance Green's function are given by

$$\tilde{Z}_{11} = N_z^2 \tilde{Z}_m + N_x^2 \tilde{Z}_e$$

$$\tilde{Z}_{12} = (\tilde{Z}_m - \tilde{Z}_e) N_x N_z = \tilde{Z}_{21}$$

$$\tilde{Z}_{22} = N_x^2 \tilde{Z}_m + N_z^2 \tilde{Z}_e \quad (5)$$

where

$$N_x = \alpha/\sqrt{\alpha^2 + \beta^2} \qquad N_z = \beta/\sqrt{\alpha^2 + \beta^2} \quad (6)$$

$$\tilde{Z}_m = \frac{1}{Y_{TM0} + Y_{TM} \coth \gamma_m h}$$

$$\tilde{Z}_e = \frac{1}{Y_{TE0} + Y_{TE} \coth \gamma_e h} \quad (7)$$

and

$$Y_{\mathrm{TM0}} = \frac{j\omega\epsilon_0}{\gamma_0} \qquad Y_{\mathrm{TE0}} = \frac{\gamma_0}{j\omega\mu_0}$$
$$\gamma_0 = \sqrt{\alpha^2 + \beta^2 - \omega^2\mu_0\epsilon_0}. \tag{8}$$

b) Magnetic Bias in z Direction: Following the above steps for a magnetic bias in z direction, the wave immittances yield:

$$Y_{\mathrm{TE}} = \frac{(\beta^2\mu_\Delta + \alpha^2\mu_z)\gamma_e + \alpha\mu_z\kappa(\alpha^2 + \beta^2)/\mu}{j\omega\mu_0\mu_z\mu_\Delta(\alpha^2 + \beta^2)} \tag{9}$$

$$Y_{\mathrm{TM}} = j\omega\epsilon_0\epsilon_r/\gamma_m \tag{10}$$

with

$$\gamma_{m,e} = \left(-\frac{q_{m,e}}{2} + \sqrt{\left(\frac{q_{m,e}}{2}\right)^2 + \left(\frac{p_{m,e}}{3}\right)^3}\right)^{1/3} + \left(-\frac{q_{m,e}}{2} - \sqrt{\left(\frac{q_{m,e}}{2}\right)^2 + \left(\frac{p_{m,e}}{3}\right)^3}\right)^{1/3} \tag{11}$$

and

$$q_m = \frac{2}{27}a^3 - \frac{ab}{3} + c \qquad p_m = b - \frac{a^2}{3}$$
$$q_e = -k_0^2\mu_z\epsilon_r\kappa\alpha/\mu \qquad p_e = (k_0^2\mu_z\epsilon_r - \alpha^2 - \beta^2\mu_z/\mu)$$
$$a = -k_0^2\epsilon_r\kappa/2 \qquad b = k_0^2\mu_z\epsilon_r - \alpha^2 - \beta^2$$
$$c = k_0^2\epsilon_r\kappa(\alpha^2 - \mu_z\epsilon_r)/\alpha. \tag{12}$$

c) Magnetic Bias in x Direction: If a magnetic bias is supplied in x direction, $\gamma_{m,e}$ have the same expression as in (11), but with different $q_{m,e}$ and $p_{m,e}$, which are given by

$$q_m = k_0^2\epsilon_r\kappa\beta/2 \qquad p_m = k_0^2\mu_x\epsilon_r - \alpha^2 - \beta^2$$
$$q_e = k_0^2\epsilon_r\kappa\beta/\mu \qquad p_e = (k_0^2\epsilon_r - \alpha^2/\mu - \beta^2). \tag{13}$$

Moreover, α and β need to be exchanged in (9), and μ_z is replaced by μ_x.

2. Bi-Anisotropic Substrate

The common way to characterize the bi-anisotropic structure of Fig. 1(b) is to assume that each layer has diagonal permittivity and permeability tensors of the form [10]:

$$\langle\vec{\epsilon}\rangle = \epsilon_0\begin{pmatrix}\epsilon_x & 0 & 0\\ 0 & \epsilon_y & 0\\ 0 & 0 & \epsilon_z\end{pmatrix} \qquad \langle\vec{\mu}\rangle = \mu_0\begin{pmatrix}\mu_x & 0 & 0\\ 0 & \mu_y & 0\\ 0 & 0 & \mu_z\end{pmatrix} \tag{14}$$

Following the above procedure, the transverse propagation constants and associated wave immittances of the bi-anisotropic substrate read:

$$\gamma_m^2 = \left(\frac{\epsilon_x}{\epsilon_y}\alpha^2 + \frac{\epsilon_z}{\epsilon_y}\beta^2\right) - \frac{\omega^2\mu_0\epsilon_0\mu_x\mu_z(\epsilon_x\alpha^2 + \epsilon_z\beta^2)}{\mu\alpha^2 + \mu_z\beta^2} \tag{15}$$

$$\gamma_e^2 = \left(\frac{\mu_x}{\mu_y}\alpha^2 + \frac{\mu_z}{\mu_y}\beta^2\right) - \frac{\omega^2\mu_0\epsilon_0\epsilon_x\epsilon_z(\mu_x\alpha^2 + \mu_z\beta^2)}{\epsilon_x\alpha^2 + \epsilon_z\beta^2} \tag{16}$$

$$Y_{TM} = \frac{j\omega\epsilon_0\epsilon_x\epsilon_z}{\gamma_m}\frac{(\mu\alpha^2 + \mu_z\beta^2)}{(\mu_x\epsilon_z\alpha^2 + \mu_z\epsilon_x\beta^2)} \tag{17}$$

$$Y_{TE} = \frac{\gamma_e}{j\omega\epsilon_0\mu_x\mu_z}\frac{(\mu_z\epsilon_x\alpha^2 + \mu_x\epsilon_z\beta^2)}{(\epsilon_x\alpha^2 + \epsilon_z\beta^2)} \tag{18}$$

3. Metallization

After obtaining the dyadic Green's function of a multilayered substrate by applying SDIA [13], the function is modified by considering a complex boundary condition [17] to incorporate the finite thickness of the conductor. If the thickness t of the strip is greater than three penetration depths, the surface impedance $Z = \sqrt{\omega\mu_o/2\sigma}$ is adequately represented by the real part of the wave impedance [3]. If t is less than three penetration depths, a better boundary condition is given by $Z = 1/(t\sigma)$ [17], where the conductivity $\sigma = \sigma_c$ is real for conventional conductors. These approximations have been verified for practical metallization thicknesses by comparison with rigorous mode-matching results [21]. For superconductors, a complex conductivity of the form [3], [17]

$$\sigma = \sigma_n(T/T_c)^4 + (1 - (T/T_c)^4)/(j\omega\mu_0\lambda_{\mathrm{eff}}^2) \tag{19}$$

is considered, which is based on the two-fluid model to approximate the H-field wave equation obtained from Maxwell and London equations [17], [22]. In (19), σ_n is often associated with the normal state conductivity at temperature T_c, and λ_{eff} is the effective field penetration depth.

Once the modified dyadic Green's function has been obtained, the dispersion and loss behavior of a given line structure is obtained by applying Galerkin's procedure. The tangential current density or the tangential electric field in the spectral domain is expanded in a set of Bessel functions, which take the edge singularities into consideration, thus leading to current distributions as shown in, e.g., [23]. On a RISC 6000/530 workstation, the calculation of the complex propagation constants, which are determined by the roots of the characteristic equation, takes 10–20 seconds per frequency sample.

III. Results

Comparisons between the results obtained with this theory and previously published data are shown in Fig. 2. The purpose of this comparison is, first, to verify the presented theory and, secondly, to demonstrate that the approach of identical transverse propagation constants given in [16] is fairly limited.

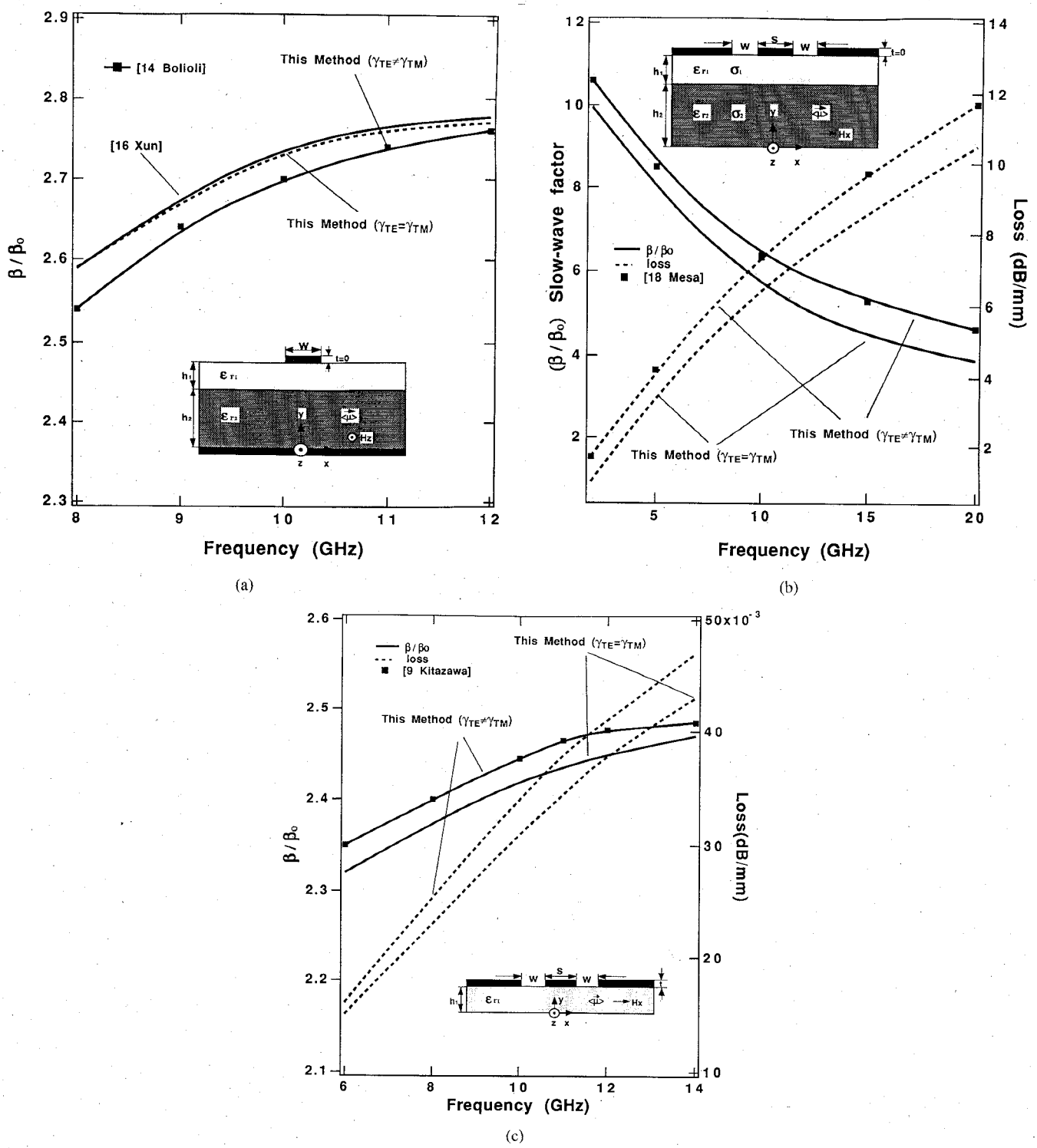

Fig. 2. Comparison of the results of this technique with data obtained by different methods. (a) Normalized propagation constant with biasing field Ho in z direction. Dimensions: $h_1 = 0.254$ mm, $h_2 = 1.150$ mm, $w = 0.9$ mm, $4\pi M_{\max} = 1740$ G, $4\pi M_S = 2300$ G, $\epsilon_{r2} = 16.6$, $\epsilon_{r1} = 9.9$. (b) Slow-wave factor and attenuation constant for multilayered CPW with ferrite magnetized in x direction. Dimensions: $s = 0.12$ mm, $w = 0.1$ mm, $h_1 = 1$ μm, $h_2 = 0.1$ mm, $\epsilon_{r1} = 14.9$, $\epsilon_{r2} = 4.3$, $\sigma_1 = 0$, $\sigma_2 = 0.1$ S/mm, $4\pi M_S = 725$ G, $H_x = 500$ Oers, $\Delta H = 37$ Oers. Superconductor: $T/Tc = 0.5$, $\lambda_{\text{eff}} = 1500$ Å, $\sigma_n = 210$ S/mm. (c) Propagation characteristics of CPW with magnetized ferrite. Dimensions: $h = 1$ mm, $w = 1$ mm, $s = 0.5$ mm, $\epsilon_r = 11.6$, $M_s = 1800$ A/cm, $H_x = 300$ A/cm. Superconductor: $T/Tc = 0.5$, $\lambda_{\text{eff}} = 1500$ Å, $\sigma_n = 210$ S/mm, $t = 0.04$ μm.

At the example of a microstrip line on layered ferrite-dielectric substrate with magnetic bias in z direction, Fig. 2(a) demonstrates the limitations of the $\gamma_{TE} = \gamma_{TM}$ approach. Close agreement with [16] can only be obtained if we restrict our method to exactly that case (dashed line). The rigorous solution derived in this paper ($\gamma_{TE} \neq \gamma_{TM}$), however, yields results which are two percent lower and which are found to be in excellent agreement with the data given in [14].

The backward-wave characteristics of a coplanar waveguide on a lossy ferrite-dielectric layered substrate for MMIC applicability are shown in Fig. 2(b). Using our rigorous approach ($\gamma_{TE} \neq \gamma_{TM}$), both the slow-wave factor and the loss behavior are in excellent agreement with values presented in [18] for the case of infinitely thin conductors. Whereas, in comparison, the method proposed in [16] ($\gamma_{TE} = \gamma_{TM}$) shows up to 20 percent deviation.

Fig. 2(c) shows a comparison with Kitazawa's data [9] for a conventional coplanar waveguide with finite conductor thickness on a single-layered ferrite substrate. The ferrite is magnetically biased in x direction. In order to realistically approximate the ideal-conductor case (no losses) in [9], a superconductor of identical thickness is assumed here. Again, close agreement is obtained with the rigorous solution presented in this paper, while the $\gamma_{TE} = \gamma_{TM}$ approach suggested in [16] leads to significant deviations. Fig. 2(c) also displays the differences obtained for the loss characteristics.

The backward-wave characteristics of a microstrip line on ferrite-dielectric substrate is shown in Fig. 3. In this case, a very thin superconductor $YBa_2Cu_3O_7$ (YBCO) is introduced for the center conductor while a conventional conductor is used as ground plane. The results demonstrate the increase of the propagation constant caused by the kinetic inductance associated with the superconductor current. As the thickness of the superconducting layer decreases, the fractional amount of magnetic energy stored in the superconductor increases, hence increasing the slow-wave factor as well as the losses. A similar behavior can be observed for the forward wave.

Backward-wave properties of the conductor-backed CPW structure on lossy ferrite-dielectric substrate are shown in Fig. 4. The high-Tc superconductor (copper is shown for comparison) is imposed on a thin dielectric substrate which is assumed to be $LaAlO_3$ with $\epsilon_r = 23$. While for the same conductor thickness, the slow-wave factor using a superconductor is only slightly larger than that of a copper conductor, considerably lower losses are obtained, as expected.

To illustrate the general applicability of the approach presented in this paper, the propagation characteristics of a microstrip line with a superconductor printed on bi-anisotropic substrate is shown in Fig. 5. The three different combinations of the tensor elements demonstrate the anisotropic effects on the propagation constant and the loss factor. As expected, the anisotropic effects increase with

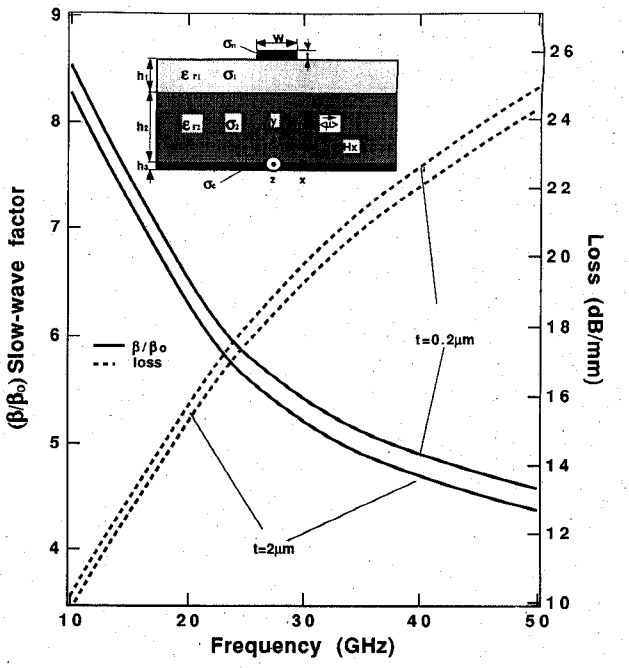

Fig. 3. Slow-wave factor and attenuation constant for multilayered microstrip line with magnetic bias in x direction. Dimensions: $w = 0.1$ mm, $h_1 = 1$ μm, $h_2 = 0.1$ mm, $h_3 = 0.5$ μm, $\epsilon_{r1} = 16.6$, $\epsilon_{r2} = 9.9$, $\sigma_c = 40$ S/m, $\sigma_1 = 0.1$ S/m, $\sigma_2 = 0.1$ S/mm, $4\pi M_s = 870$ G, $H_x = 2200$ Oers, $\Delta H = 50$ Oers. Superconductor: $T/Tc = 0.5$, $\lambda_{eff} = 1500$ Å, $\sigma_n = 210$ S/mm.

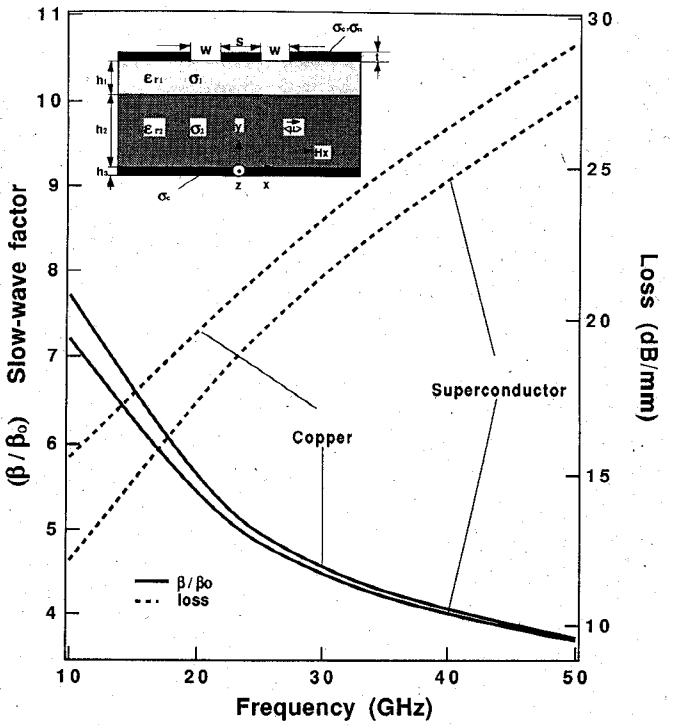

Fig. 4. Slow-wave factor and loss characteristics of multilayered CPW with magnetic bias in x direction. Dimensions: $s = 0.12$ mm, $w = 0.1$ mm, $h_1 = 1$ μm, $h_2 = 0.1$ mm, $h_3 = 0.5$ μm, $\epsilon_{r1} = 12$, $\epsilon_{r2} = 23$, $\sigma_c = 40$ S/mm, $\sigma_1 = 0.4$ S/m, $\sigma_2 = 0.1$ S/mm, $4\pi M_s = 14\,300$ G, $H_x = 770$ G, $\Delta H = 10$ Oers. Superconductor: $T/Tc = 0.5$, $\lambda_{eff} = 1500$ Å, $\sigma_n = 210$ S/mm, $t = 0.1$ μm.

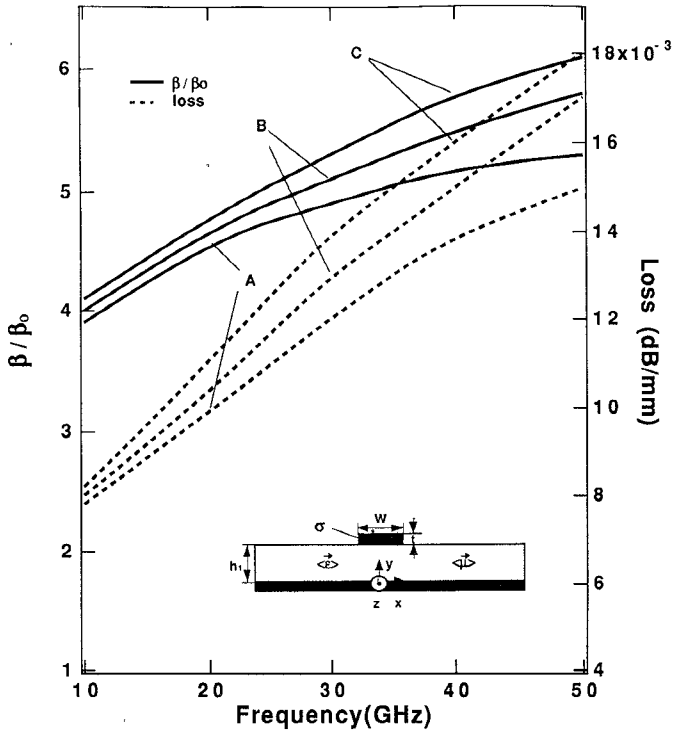

Fig. 5. Propagation characteristics of superconductor microstrip line with bi-anisotropic substrate. Dimensions: w = 1.27 mm, t = 0.04 μm, h_1 = 1.0 mm, T/Tc = 0.5, λ_{eff} = 1500 Å, σ_n = 210 S/mm. A: ϵ_x = 3.5, ϵ_y = 4.5, ϵ_z = 5.5, μ_x = 3.5, μ_y = 5.5, μ_z = 4.0. B: ϵ_x = 4.5, ϵ_y = 5.5, ϵ_z = 6.5, μ_x = 4.5, μ_y = 5.5, μ_z = 6.0. C: ϵ_x = 5.5, ϵ_y = 6.5, ϵ_z = 7.5, μ_x = 5.5, μ_y = 6.5, μ_z = 7.0.

frequency and, therefore, need to be considered in the design of high-frequency MMICs.

IV. Conclusion

The SDIA-based algorithm to rigorously derive the impedance Green's function in the spectral domain includes the following features and advantages which are essential for the reliable analysis of MMIC structures on multilayered anisotropic substrates:

Obtaining closed form expressions for the different transverse propagation constants and related immittances of the decoupled TE and TM waves in the spectral domain, thus placing no restrictions on the size of tensor elements of anisotropic or bi-anisotropic substrates.

Significantly simplifying the analysis procedure for (M)MIC structures with finite metallization thickness on multilayered anisotropic media.

Including a variety of losses caused by dielectric and ferrite materials as well as by conventional metal or high-Tc superconductors.

Since this technique combines the analysis capabilities of many previously presented methods while preserving flexibility and closed-form expressions, it offers a powerful and attractive alternative in CAD procedures for modern MMIC applications.

References

[1] R. C. Hansen, "Antenna application of superconductors," *IEEE Trans. Microwave Theory Tech.*, vol. 39, pp. 1508–1512, Sept. 1991.

[2] C. M. Chorey, K. S. Kong, K. B. Bhasin, J. D. Warner, and T. Itoh, "YBCO superconducting ring resonators at millimeter-wave frequencies," *IEEE Trans. Microwave Theory Tech.*, vol. 39, pp. 1480–1487, Sept. 1991.

[3] D. Nghiem, J. T. Williams, and D. R. Jackson, "A general analysis of propagation along multiple-layer superconducting stripline and microstrip transmission lines," *IEEE Trans. Microwave Theory Tech.*, vol. 39, pp. 1553–1565, Sept. 1991.

[4] N. G. Alexopoulos, "Integrated-circuit structures on anisotropic substrates," *IEEE Trans. Microwave Theory Tech.*, vol. MTT-33, pp. 847–881, Oct. 1985.

[5] M. Horno, "Quasistatic characteristics of microstrip on arbitrary anisotropic substrates," *Proc. IEEE*, vol. 68, pp. 1033–1034, Aug. 1980.

[6] S. K. Koul and B. Bhat, "Inverted microstrip and suspended microstrip with anisotropic substrates," *Proc. IEEE*, vol. 70, pp. 1230–1231, Oct. 1982.

[7] A-M. A. El-Sherbiny, "Hybrid mode analysis of microstrip lines on anisotropic substrates," *IEEE Trans. Microwave Theory Tech.*, vol. MTT-29, pp. 1261–1265, Dec. 1981.

[8] H. Yang and N. G. Alexopoulos, "Uniaxial and biaxial substrate effects on finline characteristics," *IEEE Trans. Microwave Theory Tech.*, vol. MTT-35, pp. 24–29, Jan. 1987.

[9] T. Kitazawa and T. Itoh, "Asymmetrical coplanar waveguide with finite metallization thickness containing anisotropic media," *IEEE Trans. Microwave Theory Tech.*, vol. 39, pp. 1426–1433, Aug. 1991.

[10] T. Q. Ho and B. Beker, "Spectral-domain analysis of shielded microstrip lines on biaxially anisotropic substrates," *IEEE Trans. Microwave Theory Tech.*, vol. 39, pp. 1017–1021, June 1991.

[11] C. M. Krowne, "Fourier transformed matrix method of finding propagation characteristics of complex anisotropic layered media," *IEEE Trans. Microwave Theory Tech.*, vol. MTT-32, pp. 1617–1625, Dec. 1984.

[12] L. Mesa, R. Marques and M. Horno, "A general algorithm for computing the bidimensional spectral Greens dyad in multilayered complex bianisotropic media: The equivalent boundary method," *IEEE Trans. Microwave Theory Tech.*, vol. 39, pp. 1640–1649, Sept. 1991.

[13] T. Itoh, "Spectral domain immittance approach for dispersion characteristics of generalized printed transmission lines," *IEEE Trans. Microwave Theory Tech.*, vol. MTT-28, pp. 733–736, July 1980.

[14] S. Bolioli, H. Benzina, H. Baudrand, and B. Chan, "Centimeter-wave microstrip phase shifter on a ferrite-dielectric substrate," *IEEE Trans. Microwave Theory Tech.*, vol. 37, pp. 698–705, Apr. 1989.

[15] M. Geshiro and T. Itoh, "Analysis of double-layered finlines containing a magnetized ferrite," *IEEE Trans Microwave Theory Tech.*, vol. MTT-35, pp. 1377–1381, Dec. 1987.

[16] P. Xun, "Spectral-domain immittance approach for the propagation constants of unilateral finlines with magnetized ferrite substrate," *IEEE Trans. Microwave Theory Tech.*, vol. 37, pp 1647–1650, Oct 1989.

[17] J. M. Pond, C. M. Krowne, and W. L. Carter, "On the application of complex resistive boundary conditions to model transmission lines consisting of very thin superconductors," *IEEE Trans. Microwave Theory Tech.*, vol. 37, pp. 181–190, Jan. 1989.

[18] F. Mesa, R. Marques and M. Horno, "Rigorous analysis of nonreciprocal slow-wave planar transmission lines," in *Proc. 21st European Microwave Conf.*, pp. 229–234, Sept. 1991.

[19] G. Cano, F. Medina and M. Horno, "Efficient spectral domain analysis of generalized multistrip lines in stratified media including thin, anisotropic, and lossy substrates," *IEEE Trans. Microwave Theory Tech.*, vol. 40, pp. 217–227, Feb. 1992.

[20] T. Q. Ho and B. Beker, "Analysis of bilateral fin-lines on anisotropic substrates," *IEEE Trans. Microwave Theory Tech.*, vol. 40, pp. 405–409, Feb. 1992.

[21] W. Heinrich, "Full-wave analysis of conductor losses on MMIC transmission lines," *IEEE Trans. Microwave Theory Tech.*, vol. 38, pp. 1468–1472, Oct. 1990.

[22] D. M. Sheen, S. M. Ali, D. E. Oates, R. S. Withers, and J. A. Kong, "Current distribution, resistance, and inductance for superconducting strip transmission lines," *IEEE Trans. Applied Superconductivity*, vol. 1, pp. 108–115, June 1991.

[23] S. M. El-Ghazaly, R. B. Hammond, and T. Itoh, "Analysis of superconducting microwave structures: Application to microstrip lines," *IEEE Trans. Microwave Theory Tech.*, vol. 40, pp. 499–508, Mar. 1992.

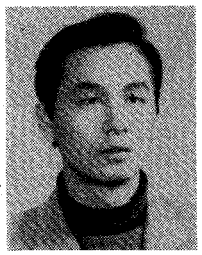

Zhenglian Cai was born in Nanjing, People's Republic of China, in 1960. He received the B.S. and M.S. degrees in electrical engineering from the Radio Department, Beijing Normal University, in 1983 and 1986, respectively.

From 1986 to 1989, he was a Lecturer and was involved in the research of millimeter waveguide filters in Electrical Engineering Department at Beijing Institute of Technology, China. From 1989 to 1990, he worked at Satellite Communications Company, Chinese Academy of Sciences, where, as a project manager, he was engaged in the design and development of low noise amplifier, C/Ku-band antennas and TV receiving systems. Since 1990, he has been a Research Assistant in the Department of Electrical and Computer Engineering, University of Victoria, Victoria, BC, Canada, working towards the Ph.D. degree. His research deals mainly with the analysis and modeling of MMIC circuits, anisotropic structures and applications of superconducting patch antennas.

Jens Bornemann (M'87–SM'90) was born in Hamburg, Germany, on May 26, 1952. He received the Dipl.-Ing. and the Dr.-Ing. degrees, both in electrical engineering, from the University of Bremen, Germany, in 1980 and 1984, respectively.

From 1980 to 1983, he was a Research and Teaching Assistant in the Microwave Department at the University of Bremen, working on quasi-planar waveguide configurations and computer-aided E-plane filter design. After a two year period as a consulting engineer, he joined the University of Bremen again, in 1985, where he was employed at the level of Assistant Professor. Since April 1988, he has been with the University of Victoria, Victoria, BC, Canada, where he is currently a Professor in the Department of Electrical and Computer Engineering. His research activities include microwave/millimeter-wave components and systems design, and problems of electromagnetic field theory in integrated circuits and radiating structures.

Dr. Bornemann was one of the recipients of the A. F. Bulgin Premium of the Institution of Electronic and Radio Engineers in 1983. He is a Fellow of the British Columbia Advanced Systems Institute. He serves on the editorial board of the IEEE TRANSACTIONS ON MICROWAVE THEORY AND TECHNIQUES, and has authored and coauthored more than 70 technical papers. Dr. Bornemann is a Registered Professional Engineer in the Province of British Columbia, Canada.